Desalination and Water Treatment
www.deswater.com
doi: 10.1080/19443994.2013.779420

51 (2013) 4271–4282
June

Taylor & Francis
Taylor & Francis Group

Influence of the water height in aeration regimes with the same membrane diffuser on technical characteristics of aeration system

Miroslav Stanojević[a], Mirjana Ševaljević[b,*], Stojan Simić[c], Miladin Ševaljević[d]

[a]*Faculty of Mechanical Engineering, University of Belgrade, Kraljice Marije 16, Belgrade, Serbia*
[b]*Technical College of Applied Science in Zrenjanin, Đorđa Stratimirovića 22, Zrenjanin, Serbia*
Email: sevaljevic.mirjana@gmail.com
[c]*Oil Refinery a.d., Modriča, Bosnia and Herzegovina*
[d]*High Technical School, Zrenjanin, Serbia*

Received 2 December 2011; Accepted 7 February 2013

ABSTRACT

Deciding on an aeration system technical characteristicssuch as energy efficiency of oxygen transport in refinery waste water and capacity of oxygen introduction is an important question. With the same membrane air distributor, in the same examined range of waste motor oil contents 5 and 10 gm^{-3} and air flows 2, 6 and 10 $m^3 h^{-1}$ energy efficiency of oxygen transport is better up to 54% and twice the real capacity of oxygen introduction, in the water column 2 m high, compared to water column 1 m high. The improvement of technical characteristics is achieved in the aeration regimes with the longer retention time between air input and output and minimal electrons density in the gas bubbles. In our paper it is proposed, electrons flux controls the oxygen transport volumetric coefficient, which determines the technical characteristics of aeration system.

Keywords: Membrane air distributor; Water column height; Active and passive oxygen transport coefficients; Electrons density state; Electrons retention molar times; Oxygen potential energy; Oxygen transport molar work; Oxygen surface molar polarization

1. Introduction

This paper examines technical characteristics of the membranes' air distributor, energy efficiency of the oxygen transport in refinery waste water at the same range of waste motor oil content 5 and 10 gm^{-3} and air flow, 2, 6 and 10 $m^3 h^{-1}$ depending on water column height 1 and 2 m. Some of the technical indicators of the aeration process installations, stated in the literature and in technical documentations of the producers, for conditions of the clean water aeration are supplied. When the aeration system is designed, it is necessary to use most efficient aeration devices. Experimental method for determination of technical membranes' characteristics is described in previous papers [1–3] based on the material balance of the aeration process [4,5].

According to the literature [4–16], the used membrane air distributor influences dominantly the technical characteristics of aeration systems.

*Corresponding author.

Membranes in Drinking and Industrial Water Treatment—MDIW 2010, June 27–30, 2010, Trondheim, Norway

The relative real aeration technical characteristics are strongly dependent on the water column height. The increasing of the real technical characteristic—energy efficiency of oxygen transport, in the water column 2 m relative to 1 m is obtained:

- Up to 60% at minimal air flow $2\,m^3\,h^{-1}$ where saturation rates controlled oxygen diffusion rate constants and oxygen volume transport coefficients.
- About 80% at the maximal air flow $10\,m^3\,h^{-1}$ in water with less added oil content, $5\,gm^{-3}$ and 25% with $10\,m^3\,h^{-1}$ where maximal oxygen transport efficiency controls the saturation rates.
- And 18–32% at the middle air flow $6\,m^3\,h^{-1}$ where the oxygen introduction volume coefficients limited with oxygen saturation rate constant as catalyst in the possible water couple reaction.

In our paper, it is proposed that the aerated oxygen can activate coupled electrons and oxygen transport in the galvanic cells depending on the oxygen chemical affinity between the polarized inter-metallic surfaces of the deposited alloys and gas bubbles, and between gas bubbles on air input and condensation nuclei on air output.

If the reduced metal atoms are present, equal anode and cathode chemical exchange electron currents of the present reduced metal atoms can be induced on the stationary corrosion potentials [17]:

- On Fe with the small hydrogen over-potential, 0.08 V and oxygen over-potential 0.25 V.
- On the inter-metals alloying and successive doping with the atoms which increase the hydrogen over-potential (Cu and Cd at 0.48 V, and Pb 0.64 V) and the oxygen over-potential (Cd 0.43 and Pb 0.31 V).

Vayenas and co-workers [18] investigated the efficiency of the hydrogen and oxygen chemical depolarization rates, relative to the Faraday depolarization rate as a measure of the modified Faraday gain, with the non-Faraday modification of the catalytic activity (NEMCA) effect, Λ in the inter-metal contact surfaces with the hypo-hyper–d-electrons transition. In this paper, it is proposed that NEMCA effect occur by a back-spillover mechanism where components active in hydrogen striping migrate from solid electrolyte onto the gas exposed electrode surface. This effect can influence overall oxygen transport coefficient in liquid to be limited with saturation or (and) diffusion step, depending on electrons density on gas bubbles diameter where van der Waals interactions are relevant in the oxygen transport activation energy, along with electrostatic interactions on hydriding/dehydriding cycles.

$$\begin{aligned}\Lambda_H \times \tfrac{I}{2F} &= \frac{dn_{H_2}}{d\tau}\\ \Lambda_O \times \tfrac{I}{2F} &= \frac{dn_{O_2}}{d\tau}\end{aligned} \tag{1.1}$$

Then the efficiencies of the Faraday electrons activated with the air flow, in contact with reduced oxygen molecules and positive hydrogen ions determine:

- chemisorbed oxygen electrons exchange current efficiency,

$$\beta(I_{O_2-/O_2}) : \beta(I_{O_2-/O_2}) = I_{O_2-/O_2}/I_F$$

- oxygen electrons chemical potential efficiency,

$$\beta(U_{O_2-/O_2}) : \beta(U_{O_2-/O_2}) = U_{O_2-/O_2}/U_F$$

- and oxygen electrons chemical power efficiency,

$$\beta_P.(I_{O_2-/O_2} \times U_{O_2-/O_2})$$

$$\beta_P = \frac{I_{O_2-/O_2}U_{O_2-/O_2}}{I_F U_F} = \beta(I_{O_2-/O_2}) \times \beta(U_{O_2-/O_2}) \tag{1.2}$$

In our previous paper, oxygen diffusion and oxygen adsorption rate constants are determined based on the oxygen transport power balance equation, depending on:

- The oxygen chemical affinity determined on the base of the Van't Hoff equation of the chemical potential equilibrium achieved after saturation time [19].
- Experimentally measured oxygen transport volumetric coefficient based on the Henry's law [1–3], described in the experimental part.

The task of this paper is to determine the dominant parameters in the control of the aeration membrane technical characteristics, depending on the water column height.

2. Experimental determination of the oxygen transport volumetric coefficient based on material balance [1–3]

The technical characteristics of membranes' air distributor for aeration by catalogue of "Gummi-Jaeger GmbH" (Deutchland) are used in various biological treatments of industry and communal waters. The type HD340 used membrane diffuser consists of the fine perforated membrane, fixed with a ring over disc of material (PP GF30) and material of membrane ethilen–propilen-dimer (EPDM). Membrane distributor can be

Table 1
Characteristics of the membrane air distributor according to catalog of the Gummi–Jaeger GmbH

Type	Dimensions			Aerated surface (m^2)	Air flow (m^3/h)	Material of disc	Material of membrane
	Diameter A total/ effective (mm)	Height-B (mm)	Height-C (mm)				
HD 270	270/220	30	58	0.037	1.5–7	PP GF30	EPDM/silicon
HD 340	340/310	46	76	0.060	2–10	PP GF30	EPDM
HD 235	240/209	32	45	0.030	1.5–7	PA GF30	EPDM
HD 325	330/290	32	45	0.059	2–10	PA GF30	EPDM
ECO 21	270*/230	24	55	0.045	1.5–7	PP GF30	EPDM
ECO 34	270*/330	24	55	0.045	2–10	PP GF30	EPDM

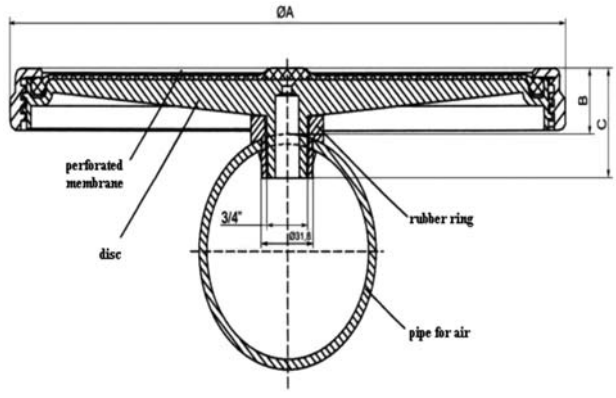

Fig. 1. The disk-shaped membrane air distributor [3].

applied on water temperature 5–35°C and air input temperature has to be less than 60°C (Table 1, Fig. 1).

The age of membrane distributor usage is 10 years and depends on wastewater characteristics and parameters of aeration process, but the control has to be made at least once per year. At standard conditions, air flow is regulated depending on oxygen demand according to recommendations for the distributor type [9,10] in the polypropylene column with dimensions $700 \times 700 \times 2200$ mm (Fig. 2).

Experimental work was performed for batch working conditions with water column 1 and 2 m high and the total volume 490 and 980 L and varying air flow of 2, 6 and 10 m^3/h. Average characteristics of wastewater in Refinery in Modriča, during the period of investigation were: pH in range 7.21–7.29, water temperature 15–25°C, oil content 13–23 mg/L, inorganic salts 0.38–0.40 mg/L, total solid matter 0.5–0.7 mg/L, chemical oxygen demand 80–180 mg/L, biological oxygen demand (BOD) to 7 mg/L, CaO 18.5–21.5 mg/L and electric conductivity 670–770 μS/cm. Characteristics of examined water are dependent on content of added motor oil 5 and 10 g/m^3, the viscous waste motor oil (SAE 15 W-40). The characteristics of added waste motor oil were: 132.0 mm^2/s viscosity index;

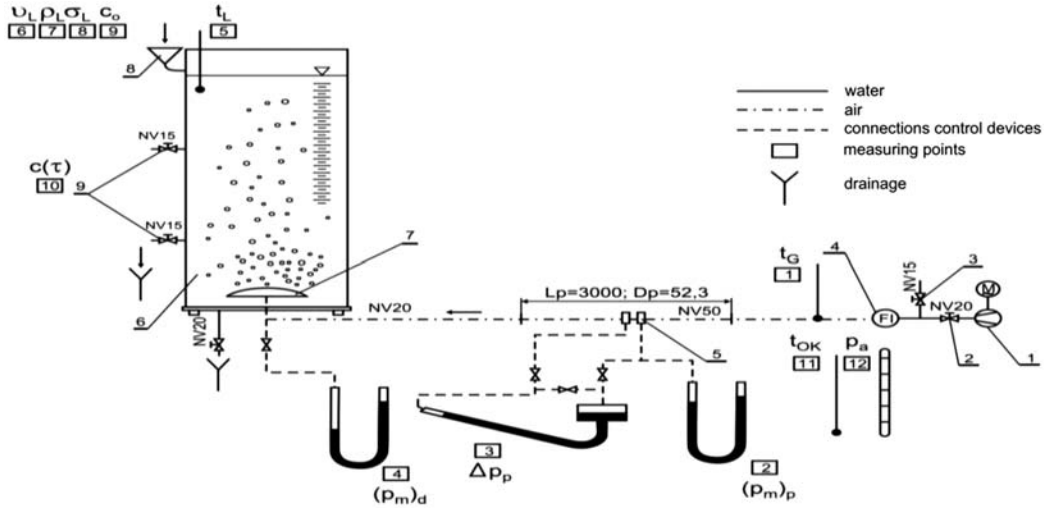

Fig. 2. The scheme of experimental installation [3]. 1—low pressure compressor (blower); 2—valve on the air inflow pipe; 3—relieving valve; 4—air flow regulator; 5—air flow measuring orifice plate; 6—column with corresponding connections and framework; 7—disk-shaped membrane air distributor; 8—water supply; 9—sampling connection.

inflammation temperature of 231.0 °C; 3.18 mg KOH/g total acid number as, 9.73 mg HCl/g total base number 0.039% Zn content; 0.310% Ca; 44.87 ppm Al and 13.4 ppm Fe; 4,11 ppm Cu and 0.98 ppm Cr.

Before starting the experiment, viscosity, density and surface tension of water in the experimental installation are determined and also the temperature of the surrounding air and water in column. Densities of three examined samples of water were in range of 992–996 kg/m^3, viscosity in range of 0.81×10^{-6}–0.99×10^{-6} m^2/s and surface tension coefficients were 76.2, 64.8 and 57.3 mN/m, respectively. The over-pressure value before $(p_m)_d$ and after the orifice plate $(p_m)_p$ was measured when the first air bubble entered in the water.

Dissolved oxygen was previously removed using a calculated concentration of sodium-sulphite, Na_2SO_3 and cobalt-chloride-hexa hydrate, $CoCl_3{\cdot}6H_2O$.

When air flow is stabilized, the dissolved oxygen content is measured until the same value is repeated thrice using Hanna Instruments 9142 with polarographic sensor, with accuracy 0.05 g/m^3, after water sampling from the column in equal time intervals ($\Delta\tau = 60$ s).

According to literature [9], the total coefficient of oxygen transfer from contact surface in liquid phase K_L, ms^{-1} and from contact surface in gas phase, K_G, ms^{-1} determines oxygen transport volumetric coefficient in liquid k_L, ms^{-1} and oxygen transport coefficient in gas phase, k_G, ms^{-1} based on the reduced Henry's constant, Ha_{red}, J mol^{-1}.

$$\frac{1}{K_L} = \frac{1}{k_L} + \frac{1}{Ha_{red} \times k_G} \tag{2.1}$$

$$\frac{1}{K_G} = \frac{1}{k_G} + \frac{Ha_{red}}{k_L} \tag{2.2}$$

$$Ha_{red} = \frac{Ha \times x}{C_L},\ \frac{Pa\ m^3}{kmol} \tag{2.3}$$

where $c_L = \frac{\rho_L}{M_L}$ kmol/m^3.

The ratio of transport coefficient in liquid and gas phase is:

$$\frac{k_L}{k_G} = (0,1 - 0,5)\ \frac{Pa\ m^3}{kmol} \tag{2.4}$$

The negligible resistance for transport in gas and reduced Henry's constant of order 10^8 equalize total, K_L and transport oxygen volumetric coefficient k_L.

$$K_L \approx k_L \tag{2.5}$$

Experimental determination was possible on the base of the material balance of oxygen in the batch reactor [6,8], applied in our experimental conditions

$$Q \times c_{in} + \dot{V}_G \times c_{ul} - V_L \times R(\tau) = Q \times c + \dot{V}_G \times c_{iz} + V_L \times \frac{dc}{d\tau} \tag{2.6}$$

$$V_L \frac{dc}{d\tau} = q(c_{ul} - c_{iz}) - V_L r(\tau) \tag{2.7}$$

The gas phase material balance equation has to be applied also.

$$\dot{V}_G \times (c_{ul} - c_{iz}) = A \times K_L \times [c^*(c_{iz}) - c] \tag{2.8}$$

$$a = \frac{A}{V_L} \tag{2.8a}$$

$$k_L a = \frac{(c_{ul} - c_{iz}) dV_G}{V_L (c^*(c_{iz}) - c) d\tau}, \frac{1}{s} \tag{2.9}$$

where $\dot{V}_G = dV_G/d\tau = q$, m^3/s—air flow; Q, m^3/s—water flow (for batch process conditions $Q = 0$); c_{in}, kg/m^3—mass concentration of oxygen in the influent, $R_{O_2}(\tau)$, kg/(m^3·s)—specific oxygen consumption during biological treatment; c, kg/m^3—mass concentration of oxygen in the liquid and effluent. $C^* = c$ (c_{iz}), kg/m^3—equilibrium mass oxygen concentration depending on partial oxygen pressure on air output. $A = a \times V_L$, m^2—total contact surface between air and water, a, m^2/m^3—specific surface of contact between air and water, c_{ul}, kg/m^3—mass concentration of oxygen in air at the input, c_{iz}, kg/m^3—mass concentration of oxygen in air at the output, V_L, m^3—water volume, R, J/kmol K—universal gas constant, Ha, Pa kmol (O_2 + L)/kmol O_2—Henry's constant oxygen distribution coefficient between air and water, T_G, K—absolute air temperature, C_L, kmol/m^3 molar concentration of water.

The combined Eqs. (2.7) and (2.8) for $K = k$ in batch conditions give:

$$\frac{dc}{d\tau} = k_L a[c^*(c_{iz}) - c] - R(\tau) \tag{2.10}$$

$$c^*(c_{iz}) = \frac{c_{iz}}{H_C} \tag{2.11}$$

Combined Eqs. (2.10) and (2.11) define oxygen concentration on air output, c_{iz} and enable determination of the oxygen transport volume coefficient on the base of the slope, m of the liner function.

$$\frac{dc}{d\tau} = k_L a\left[\frac{c_{iz}}{H_C} - c\right] - R(\tau) \tag{2.12}$$

$$c_{iz} = \frac{qc_{ul} + V_L k_L c}{q + \frac{V_L k_L a}{H_c}},\ \frac{\text{kg}}{\text{m}^3} \tag{2.13}$$

$$\frac{dc}{c_{ul} - H_c c} = \left[\frac{k_L a}{H_c + \frac{V_L}{q}} - R(\tau)\right]\tau \tag{2.14}$$

$$\ln\frac{c_{ul} - H_c c_0}{c_{ul} - H_c c(\tau)} = m\tau \tag{2.15}$$

The solving of the Eq. (2.14) enables linear function to be obtained:

- by combined Eqs. (2.12) and (2.13).

$$Y = mX \tag{2.16}$$

- by using ideal gas state equation and modified Henry's constant, *Hc*.

$$c_{ul} = \frac{p_{ul} \times M_{O_2}}{R \times T_G},\ \frac{\text{kg}}{\text{m}^3} \tag{2.17}$$

$$H_c = \frac{H_a}{RT_R c_L} \tag{2.18}$$

$$Y = \ln\frac{\frac{p_{ul}M_{O_2}}{RT_G} - \frac{\text{Ha}}{RT_R c_L}c_o}{\frac{p_{ul}M_{O_2}}{RT_G} - \frac{\text{Ha}}{RT_R c_L}c(\tau)} \tag{2.19}$$

$$X = \tau \tag{2.20}$$

$$m = \frac{\frac{\text{Ha}}{RT_R c_L}k_L a}{\frac{\text{Ha}}{RT_R c_L} + \frac{V_L}{V_G}k_L a} - R_{O_2}(\tau) \tag{2.21}$$

The values of Y experimentally obtained for each value of $c(\tau)$ in time intervals of 1 min are used in calculation of the oxygen transport rate constant, $k_L a$ acc. to the Eq. (2.21) on the base of the slope determined according to the Eq. (2.16).

$$k_L a = \frac{\text{Ha}(m + R_{O_2}(\tau))V_G}{V_G\text{Ha} - (m + R_{O_2})V_L RT_R c_L} \tag{2.22}$$

Temperature corrections factor, θ (Table 2) transforms real oxygen transport volumetric coefficient on standard conditions to $(k_L a)_s$ for $t_L = 20$°C according to literature [4]:

$$(k_L a)_s = \frac{(k_L a)_{t_L}}{\theta^{t_L - 20}},\ \frac{1}{s} \tag{2.23}$$

Table 2
Temperature correction factors

Treatment procedure	Temperature correction factor, θ	
	The range	Typical value
Active sludge	1.00–1.04	1.02
Aerated lagoon	1.04–1.12	1.08
Biological filters	1.02–1.14	1.08

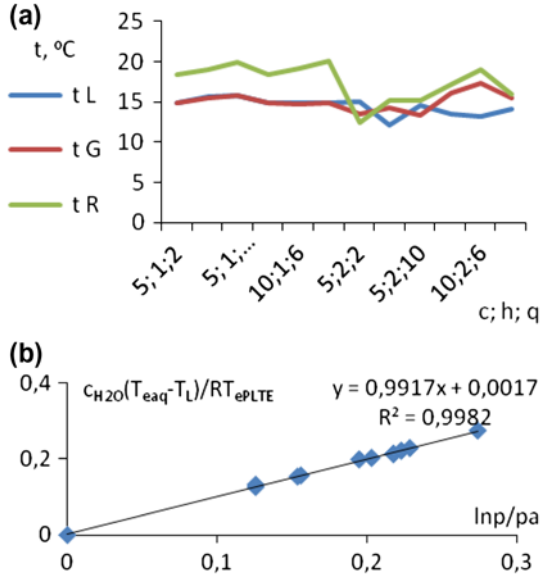

Fig. 3. (a) Diagram of liquid temperature, t_L, gas temperature t_G and temperature of rounding air, t_R, depending on the aeration regime, *c-h-q* (Table 4). (b) The functional dependence for determination of the equilibrium electrons temperatures, t_{ePLTE} in the isochoric exchanged water sensible and latent heat of adsorbed components [20], $T(e_{PTLE})_{M\times H_2O} = \frac{C_{V,L}(T(e)_{aq} - T_L)}{R\times\ln\frac{p_0}{p_a}}$.

Table 3
Technical characteristics of aeration systems [3]: depending on added motor oil, c, $g\,m^{-3}$, water column height, h, m and air flow, q, $m^3\,h^{-1}$, c-h-q: real energy efficiency [3], Ee´, g/kWh, real oxygen introduction capacity, OC´, g/h; the oxygen transport efficiency [3] E´, %; experimental determined oxygen transport volume coefficients [3], $(k_La)_m\,h^{-1}$; oxygen drift rate constant $K_{O_2}dr = 0.21\,q/VL\,h^{-1}$

Reg. c-h-q	OC´ $g\,h^{-1}$	E´ %	Ee´ $gkWh^{-1}$	$K_{O_2}dr h^{-1}$	(K_La) $m\,h^{-1}$
5-1-2	6.16	0.84	18.4	0.8	2.86
5-1-6	8.08	0.44	9.8	2.4	3.74
5-1-10	10.4	0.29	7.1	4	4.83
10-1-2	5.04	0.7	15.0	0.8	2.34
10-1-6	6.69	0.36	8.1	2.4	3.11
10-1-10	8.50	0.24	5.8	4	3.95
5-2-2	9.53	1.12	28.4	0.4	2.04
5-2-6	9.52	0.46	11.5	1.2	2.03
5-2-10	19.0	0.62	12.9	2	4.06
10-2-2	8.20	1.00	24.5	0.4	1.75
10-2-6	8.84	0.43	10.7	1.2	1.89
10-2-10	10.7	0.27	7.3	2	2.29

3. Results and discussion

The aim of this paper is to examine the technical characteristic depending on:

- The ratio of the oxygen transport volumetric and drift rate constant,
- The passive saturation and diffusion rate constants calculated in our previous paper [19],
- Electron density in couple process PLTE between electrons and hydrogen ions $y = [e]_r$, $molm^{-6}$ [20], and
- Oxygen absorption rate constants [19].

The technical characteristics are calculated based on the experimental values of the oxygen transport volume coefficient, $(k_La)_m$ obtained with the same

Table 4
The previous obtained results: the measured temperatures [3]; liquid temperature, t_L; gas temperature before air input, t_G; temperature of the rounding air, t_R, ℃ [3]; calculated electrons hydration temperature, T_{eaq} [20] $T_{eaq} = \frac{RT_L \ln c(O_2)_L}{\Delta S^{\theta}(H_2O)_L}$ (3.1), $\Delta S^{\theta}(H_2O)_L = 69.9\,J\,mol^{-1}\,K^{-1}$; calculated the electrons temperature in partial local equilibrium, T_{ePLTE} exchanging latent heat $T_{ePLTE} = \frac{C_{V,L}(T_{eaq}-T_L)}{R\ln\frac{P_o}{P_a}}$ (3.1a)

c-h-q	t_L (℃) [3]	t_G (℃) [3]	t_R (℃) [3]	$t_L - t_G$ (℃)	t_{eaq} (℃) [19]	t_{ePLTE} (K) [19]
5-1-2	14.9	14.9	18.4	0	$16 \approx \frac{t_G+t_R}{2}$	79.3
5-1-6	15.6	15.6	19	0	$16 \approx \frac{t_G+t_R}{2}$	23.2
5-1-10	15.8	15.8	19.9	0	$20.3 \geqslant t_R$	191.5
10-1-2	14.9	14.9	18.4	0	$21.7 \geqslant t_R$	480
10-1-6	14.8	14.8	19.2	0	$21.7 \geqslant t_R$	378.4
10-1-10	14.9	14.9	20.1	0	$21.7 \approx t_R$	284
5-2-2	15	13.5	12.5	1.5	$16.35 \geqslant t_L$	68.5
5-2-6	12.1	14.3	15.2	−3.1	$13 = \frac{t_G+t_L}{2}$	41
5-2-10	14.5	13.4	15.3	1.1	$13.1 \approx t_G$ 66	5.1E4 1E6
10-2-2	13.5	16.2	17.2	−2.7	$20.6 > t_R$	318
10-2-6	13.2	17.4	19.1	−4.2	$20.6 > t_R$	294
10-2-10	14.1	15.5	16	−1.4	$18 > t_R$, 38	129 798

membrane diffuser according to equations given in the appendix part, (a). The oxygen transport volumetric coefficients are calculated also according to chosen empirical models given in the supplementary part (b). These parameters are determined depending on aeration regime defined with the added oil content c; water column height, h and air flow, q, i.e. denoted as c-h-q [3] (Fig. 3(a) and (b), Tables 3–5).

In the aeration regimes with the minimal air flow, c-h-2, the measured oxygen transport volume coefficients indicate the agreement with the oxygen transport volume coefficients and empirical calculated according to Kawase model, based also on the surface tension and water column height, along with molecular oxygen diffusion coefficient and liquid viscosity (Table 5, Fig. 4).

The relative technical parameters based on the real oxygen coefficient of volume transport, $R_{act} = (k_L a/k_{dr})_2/(k_L a/k_{dr})_1$ are maximal in the regime 5-2-10 where the relative oxygen chemical energy transport parameter, $R_{pas} = (k_s/k_d)_2/(k_s/k_d)_1$ is minimal (Table 6, Fig. 5).

According to the Lingane equation, (3.2), oxygen diffusion rate constant at equal oxygen diffusion coefficient, D diffusion layer depth, δ and contact surface A would be decreased two times in the water volume $V_1 = 1\,m^3$ (2 m high water column) relative to the water volume, $V_2 = 0.5\,m^3$ (1 m high water column).

$$k_d = \frac{DA}{\delta V} \tag{3.2}$$

However, oxygen diffusion rate constant, k_d is less about 2.44 times (5-1-q) to 2.33 (10-2-q) (Table 5) in the water column 2 m high relative to 1 m, independently on the air flow.

Table 5
The previous obtained results: saturation rate constants k_s, h^{-1} [19]; diffusion rate constant, k_d, h^{-1} [19]; adsorption rate constant, k_a [19]; and oxygen transport volumetric coefficients calculated to the chosen models to Kawase $(k_L a)_K$ and to Calderbank $(k_L a)_C$ [3]

c-h-q	k_s (h^{-1})	k_d (h^{-1})	k_a (h^{-1})	$(k_L a)_K$ (h^{-1})	$(k_L a)_C$ (h^{-1})
5-1-2	3.2	4.7	−0.047	2.15	6.85
5-1-6	3.5	4.7	−0.047	5.68	5.06
5-1-10	5.4	4.7	−0.047	11.07	5.53
10-1-2	3.0	4.2	−0.036	2.17	7.44
10-1-6	3.7	4.2	−0.036	5.64	5.42
10-1-10	5.4	4.2	−0.036	12.61	5.1
5-2-2	2.3	1.92	−0.0084	1.59	4.67
5-2-6	2.5	1.92	−0.0084	5.17	4.50
5-2-10	3.0	1.92	−0.0084	9.83	4.69
10-2-2	2.4	1.8	−0.0026	1.65	4.97
10-2-6	2.6	1.8	−0.0026	5.21	4.95
10-2-10	3	1.8	−0.0026	9.93	5.06

Table 6
The relative characteristics of 2 m high water column to 1 m high, defined as the ratio of the examined parameter R, at equal oil content and air flow: relative real energy efficiency of oxygen transport: $R_{Ee} = E'_{e2}/E'_{e1}$; relative real capacity of oxygen introduction, $R_{OC} = OC'_2/OC'_1$; relative ratio between oxygen volumetric and drift, rate constants, $R_{act} = (k_L a/k_{dr})_2/(k_L a/k_{dr})_1$; relative oxygen transport efficiency, $R_E = E'_2/E'_1$; relative ratio of the oxygen saturation and diffusion; rate constants: $R_{pas} = (k_s/k_d)_2/(k_s/k_d)_1$

	R_{pas}	R_{Ee}	R_{OC}	R_{act}	R_E
5-h-2	1.76	1.54	1.54	1.42	1.33
5-h-6	1.76	1.17	1.18	1.1	1.04
5-h-10	1.37	1.81	1.82	1.67	2.13
10-h-2	1.87	1.6	1.64	1.49	1.43
10-h-6	1.63	1.32	1.32	1.2	1.19
10-h-10	1.3	1.25	1.25	1.16	1.12

4. Influence of the water height on the technical characteristics of aeration systems

Electrons concentration gradients control the molar electrons and oxygen fluxes rates, $v_{O2,L}$ and v_{O2dr} from the beginning up to the equivalent titration point (ettp) through equal molar contact surface $a = 1\,m^2/m^3$ through the same contact surface monolayer depth, δ, on the side of the gas $v_{O2dr}(e)$ and on the side of the liquid $v_{O2,L}(e)$, depending on the chemisorbed oxygen concentration gradients n_{O2}/δ, and, n_{O2G}/δ, as well as on the transport volumetric and drift rate constants:

$$\frac{v_{O2,L}(e)}{v_{O2dr}(e)} = \frac{k_L a \times n_{O2,L}}{k_{O2d_r} \times n_{O2G}} \tag{4.1}$$

where:

$$\frac{v_{O2,L}/n_{O2,L}}{v_{O2dr}/n_{O2G}} = \frac{k_L a}{k_{O2dr}}\ v^{\theta}_{O2,L} \times \tau_L/a = v^{\theta}_{O2dr} \times \tau_{dr} = h \tag{4.2a}$$

$$\frac{v^{\theta}_{O2,L}}{v^{\theta}_{O2dr}} = \left(\frac{k_L a}{k_{O2dr}}\right)_{c,q} = f(h) \tag{4.2b}$$

The study of dominant processes and parameters in the control of the water height influence on the technical characteristics of the aeration system (Table 3, Fig. 4). is based on the comparison between the active measured [3] and the calculated passive oxygen transport rate constants [19] as well as calculated according to the chosen models of Kawase and of Calderbank [3] (Table 5, Fig. 4).

For all the examined aeration regimes with the same membrane diffuser, the linear function based on the experimental data is obtained between the energy efficiency of oxygen transport, $y = E'_e$ g kWh^{-1} and oxygen volumetric and drift rate constants ratio, $x = k_L a/k_{O2dr}$, with the strong correlation coefficient, $R^2 = 0.9814$ (Fig. 6):

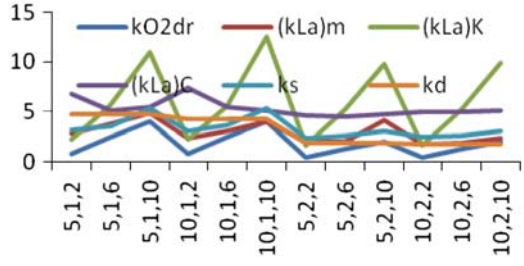

Fig. 4. The influence of examined aeration regimes on: the measured standard oxygen volumetric transport coefficients (k_La), [3], calculated values to the chosen empirical models to Kawase, $k_L a$ (K) and to Calderbank, $k_L a$ (C) [3], oxygen drift rate constant, k_{O2dr}, [19] oxygen chemical relaxation rate constant as reciprocal value of the saturation time, k_s [19] and calculated diffusion transport rate constants, k_d [19].

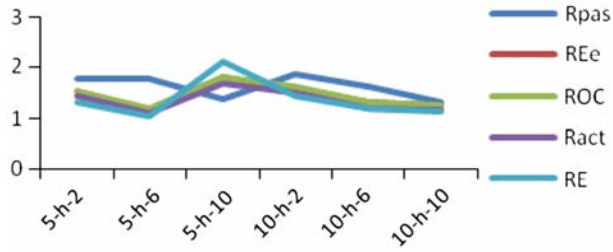

Fig. 5. The relative values of the examined technical parameters calculated at equal oil content and air flow (Table 6): relative real energy efficiency of oxygen transport: $R_{Ee} = E'_{e2}/E'_{e1}$, relative real capacity of oxygen introduction, $R_{OC} = OC'_2/OC'_1$, relative ratio between oxygen volumetric and drift, rate constants, $R_{act} = (k_L a/k_{dr})_2/(k_L a/k_{dr})_1$, relative oxygen transport efficiency, $R_E = E'_2/E'_1$ and chemical parameter: relative ratio of the oxygen saturation and diffusion, rate constants: $R_{pas} = (k_s/k_d)_2/(k_s/k_d)_1$.

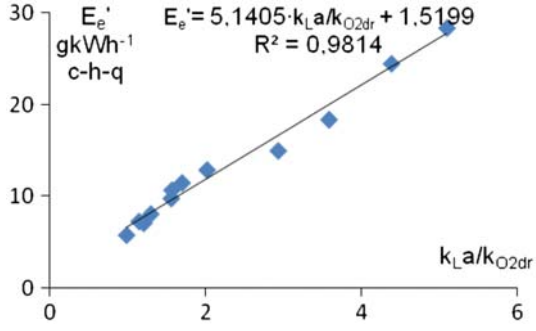

Fig. 6. Functional dependence between: real energy efficiency of oxygen transport $Y = E'_e$, $gkWh^{-1}$, and measured oxygen transport volumetric coefficient and drift rate constant ratio $(k_L a)/k_{O2dr}$, depending on the examined aeration regimes.

$$E'_e = 5.4\frac{k_L a}{k_{dr}} - 1.5199 \tag{4.3}$$

Based on the measured ratio, $\frac{k_L a}{k_{dr}}$ the energy efficiency can be calculated based on the slope, $tg\ \alpha$ in the Eq. (4.3) obtained with the same examined air distributor.

$$tg\alpha = \frac{\Delta Ee}{\Delta(k_L a/k_{O2dr})} = 5.1405\ gkWh^{-1} \tag{4.4}$$

In contact surface with depolarized hydrogen electrons flux density currents, on the side of gas equivalent with electrons density, flux on the side of liquid phase has to be achieved in equivalent titration point of component active in hydrated electrons flux energy transport (ettp).

$$\frac{v^{\theta}_{O2,L}}{v^{\theta}_{O2dr}} = \left(\frac{k_L a}{k_{O2dr}}\right)_{ettp} = 1$$

Molar electrons energy, $W^{\theta}_{k_L a=k_{dr}}$ received from the outer source up to the equivalent electrons titration point is calculated as the reciprocal value of the oxygen energy efficiency:

$$W^{\theta}_{k_L a=k_{dr}} = \frac{1}{\Delta E e'^{\theta}(\Delta(k_L a/k_{dr}) = 1)} \quad (4.5)$$

$$\Delta \mathrm{Ee}'^{\theta} = tg\alpha \times \frac{\Delta(k_L a/k_{dr})}{M_r(O_2)} = \frac{5.1405}{32}\Delta(k_L a/k_{dr}) \quad (4.5a)$$

The combined Eqs. (4.5) and (4.5a) give the molar transferred energy flux in the equivalent titrations points:

$$W^{\theta}_{k_L a=k_{dr}} = \frac{32}{5.1405}3.6 \times 10^6 = 22.41 \text{ MJ mol}^{-1} \quad (4.5b)$$

In the double electric layer, hydrated electrons activate water as heat exchanger of the sensible heat with the components depending on its affinity to electrons (oxygen, hydrogen, inorganic salts, salts composites, metals alloys):

- In the outer Helmholtz plane, $\varepsilon_{r(PbO)} = 25.9$,
- In inner Helmholtz plane, $\varepsilon_{r(CaCO3)} = 6$,

In the reaction Helmholtz plane relative electric permittivity are intermediate values:

$\varepsilon_{r(PbS)} = 17.9$,

$\varepsilon_{r(Fe2O3)} = \varepsilon_{r(PbSO4)} = 14.3$,$\varepsilon_{r(kresol)} = 11.6$, $\varepsilon_{r(J2)} = 11.2$, $\varepsilon_{r(octanol)} = 10.43$, $\varepsilon_{r(Hg2Cl2)} = 9.4$ and $\varepsilon_{r(Na2CO3)} = 8.4$, $\varepsilon_{r(dichlir–oroan)} = 10$, $\varepsilon_{r(fenol)} = 9.8$, $\varepsilon_{r(J2)} = 11.2$, $\varepsilon_{r(chinolin)} = 9$, etc. [21]. The gas component at different pressure and temperatures than standard values change the relative electric permittivity's, according to the reference [21], $(\varepsilon_r - 1)_p/(\varepsilon_r - 1)_{p0,Ts} = (p/(T_p - T_s))/(p/T_s))$: $\varepsilon_r(N_2) = 1 \pm 5$), $\varepsilon_r(H_2) = 1 \pm 3$, $\varepsilon_r(O_2) = 1 \pm 2$ and $\varepsilon_r(CO_2) = 1 \pm 1$. In the Helmholtz layer, HP, structural water changes in $CuSO_4{\cdot}5H_2O/CuSO_4$ make possible the equal relative electric permittivity of the O_2^- and of the anhydrous copper-sulfate $\varepsilon r(CuSO_4$ and $O_2-) = 10.3$ [21,22].

The specific chemisorbed components transform electrons kinetic energy into potential energy depending on the affinity to electrons:

$$\Delta_a G(O_2) = F\Delta\varphi_p$$

The unspecific adsorbed ions transform the potential energy in the oxygen impulse (in closed system) or kinetic energy (in open system) [20] $W^{\theta}_{p_{k_L a=k_{dr}}}$:

$$W^{\theta}/\varepsilon_0 = W^{\theta}(c)_{O2}/\varepsilon_0 \varepsilon r \quad (4.6)$$

$$W(c)_{O2} = \varepsilon_r \times W^{\theta}_{p_{k_L a=k_{dr}}} \times c_{O2} = F\Delta\psi \quad (4.6a)$$

In the Helmholtz plane, chemical potential relaxation work determines the difference between the potential and kinetic energy (Table 7):

$$\Delta\mu = F\Delta\chi = \Delta_a G^{\theta}(O_2) - W(c)_{O2} \quad (4.7)$$

$$F\Delta\chi/RT_0 = \frac{\Delta a G^{\theta}(O_2) - W^*(O_2)}{273.15R} \quad (4.7a)$$

In the 1 m high water column, the external energy source favours specific chemisorptions of the dissociated oxygen on the components active in endothermic heat transport due to the maximal affinities to electrons, $Ea(O/O^-) = 783 \text{ kJ mol}^{-1}$ and $Ea(O/O_2^-) = 642 \text{ kJ mol}^{-1}$.

External source keeps stationary oxygen polarization due to the exothermic affinity to electrons, $Ea(O^-/O_2^-) = -141 \text{ kJ mol}^{-1}$ equal with the difference

Table 7
The calculated data: molar oxygen affinities to electron, calculated in our previous work, $\Delta a G^{\theta}_{O2}$ [19]; molar electrons transport work in layer with the equilibrium oxygen concentration at electric permittivity $\varepsilon_r = 10.3$ acc to Eq. (4.6a); oxygen surface molar chemical energy calculated to Eq. (4.7) and compared with the gaseous pressure work on the freeze water temperature $F\Delta_\chi/RT$

c-h-q	$\Delta a G^{\theta}_{O2}$ (kJ mol^{-1})	W^*_{O2} (kJ dm^{-3})	$F\Delta_\chi/RT$ Eq. (4.7a)
5-1-2	−74.5	−70.7	−1.65
5-1-6	−36.3	$-\Delta G^{\theta}(O_2/O_2^-)_{aq}$	−1.9
5-1-10	−74.5	−69.3	−2.26
10-1-2	−70.6	−70.2	−0.17
10-1-6	−70.6	−70.2	−0.17
10-1- 10	−70.6	−70.2	−0.17
5- 2-2	−74.5	−70.2	−1.87
5-2-6	64.2	−74.2	60
5-2-10	−64.2; 1377	−70.7	2.82
10-2-2	−64.2	−72.8	3.73
10-2-6	−64.2	−73.5	4.05
10-2-10	−70.6; −1377	−72.8	0.96

Table 8
Previous determined data: stationary measured, $\gamma_{st,m}$, gm^{-3}; equilibrium oxygen contents, γ^*, gm^{-3}; electrons density in couple process PLTE between electrons and hydrogen ions $y=[e]_r$, $molm^{-6}$ [20]; and oxygen over-pressure, $x=(p_{in}-_{pa})$, Pa [3]; compared oxygen volume transport coefficient with calculated values to chosen model, active drift and passive saturation and diffusion rate constants, k, h^{-1}

c-h-q	$\gamma_{st,m}$ (g m^{-3})	γ^* (g m^{-3})	$\Delta[e]rV_L$ (mol m^{-3})	ΔP_{air} (kPa)	Compared values k (h^{-1})
5-1-2	6.40	10.1	1925	13.6	$(k_La)_m=k_s=(k_La)_K$
5-1-6	6.60	10	2100	17.1.	$(k_La)_m=k_s$
5-1-10	6.50	9.9	2083	24.3	$(k_La)_m=k_s=(k_La)_C$
10-1-2	5.80	10.1	3111	13.6.	$(k_La)_m=(k_La)_K$
10-1-6	6.00	10.1	3270	16.8	$(k_La)_m=k_s$
10-1-10	5.90	10.1	3185	24.7	$k_{O2dr}=(k_La)_m=k_d$
5-2-2	6.40	10.1	132	22.3	$(k_La)_m=(k_La)K=k_d=k_s$
5-2-6	6.70	10.6	130	25.2	$k_La)_m=k_d=k_s=2$
5-2-10	7.00	10.3	102	0.061	$(k_La)_m=(k_La)_C$ and $k_{dr}=k_d=(k_La)_m/2$
10-2-2	5.90	10.4	278	22.9	$(k_La)_m=(k_La)_K=k_d$
10-2-6	6.10	10.5	278	26.1	$(k_La)_m=k_d$
10-2-10	6.40	10.4	360	32.1	$(k_La)_m=k_d$

between the two endothermic oxygen states ($Ea(O/O^-)-Ea(O/O_2^-)=Ea(O^-/O_2^-)$. In the equivalent titration of the titrate hydrogen exothermic electrons affinity $\Delta_{dep}E(H^-/H)=-73\,kJ\,mol^{-1}$ (Table 7, regimes: 10-2-q oxygen affinities to electrons is consumed in the depolarization work of polarized chemisorbed hydrogen. In surface layer with the relative electric permittivity, $\varepsilon_r=10$, $\Delta_{dep}E(H^-/H)=Ea(O^-/O^{2-})/2=-141/2=-70.5\,kJ\,mol^{-1}$, $Ea(O/O^-)/\varepsilon_o\varepsilon_r=\Delta_{dep}E(H^-/H)/\varepsilon_o$, $E(H^-/H)=Ea(O/O^-)/\varepsilon_r=-74.5\ kJ\,mol^{-1}$ (5-1-2, 5-1-10, 5-2-2) and $Ea(O/O^{2-})/\varepsilon_o\varepsilon_r=\Delta_{dep}E(H^-/H)/\varepsilon_o$ determines the $\Delta_{dep2}E(H^-/H)=Ea(O/O^{2-})/\varepsilon_r=-64.2\ kJ\,mol^{-1}$, (5-2-6, 10-2-2- and 10-2-6) (Table 7).

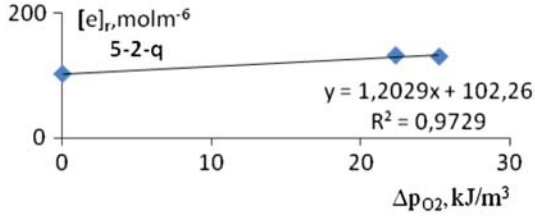

Fig. 8. The linear functional dependence in the aeration regimes 5-2-*q*, between: electrons density in couple process PLTE between electrons and hydrogen ions $y=[e]_r$, $molm^{-6}$ [20] and oxygen over-pressure, $x=(p_{in}-p_a)$, *Pa*.

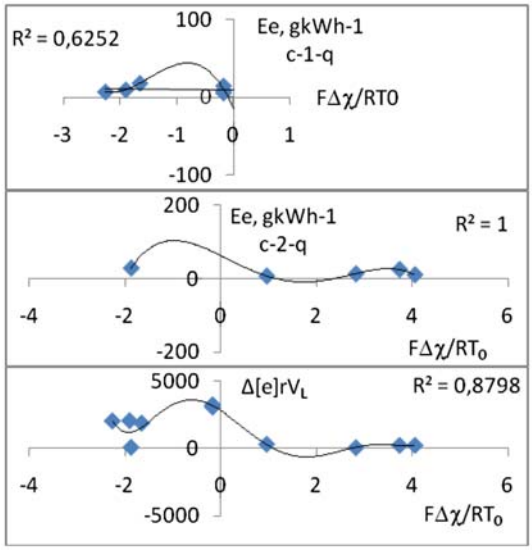

Fig. 7. The functional dependences of the real energy efficiency of oxygen transport and electrons density in gas bubbles on the oxygen surface polarization, depending on the examined the aeration regimes.

In the aeration regime 5–1-6, the stationary electrons transport energy of the chemisorbed hydrated oxygen molecules $\Delta G(O_2/O_2^-)_{aq}=31.84\,kJ\,mol^{-1}$ keep the equilibrium of spontaneous dissolved oxygen enthalpy with the endothermic titration (anode surface polarization):

$Ea(O_2/O_2^-)-G(O_2/O_2^-)_{aq}={}_{diss}H(O_2)=-11.7$ kJmol,

$E_a(O_2^-)=W^{st}(c_s)=\varepsilon_r\times W^{\theta}_{p_{k_La=k_{dr}}}c_{sO2}=43\ kJ\ mol^{-1}$.

The maximal energy efficiencies of oxygen introduction are achieved in the aeration regimes 5-2-*q* in the range of electrons densities directly proportional with the air over-pressure on the air input (Fig. 8), at the surface negative—cathode polarization, $-1.9\,RT_0$ (Table 8, Fig. 7).

5. Conclusion

The aeration plant has to be chosen based on the understanding of the water column height influence, so that real capacity of oxygen introduction corresponds to the real oxygen consumption biology oxygen demand of active sludge, at maximal energy efficiency in conventional plants. The height of the water column above the air distributor influences on the contact time between the liquid and gaseous state, i.e. how good oxygen transport efficiency will be realized with oxygen transport volume coefficient, k_La.

(a) In the 2 m high water column, *the relative technical characteristics* are increased in comparison to the 1 m high water column, depending on the air flow and waste motor oil content:

The increase in the real technical characteristic in the water column 2 m relative to 1 m is obtained:

- Up to 57% of the energy efficiency of oxygen introduction, at the minimal air flow $2\,m^3h^{-1}$,
- Eighty percent transport efficiency in water with less added oil content, $5\,gm^{-3}$at the maximal air flow, $10\,m^3h^{-1}$,
- And 18–32% at the middle air flow $6\,m^3h^{-1}$ where $k_La = k_s$.

(b) The over-pressure controls the electrons density in aeration regimes 5-2-*q*. In the quasi-reversible processes, $k_La = k_s = k_d$ in regimes 5-2-$q \leqslant 6$. the best energy efficiency of oxygen introduction is obtained for the regime 5-2-2 for 57% relative to the regime 5-1-2 due to the cathode surface polarization $F\Delta\chi_{5\text{–}2\text{–}2} = -1.9RT_0$ above $F\Delta\chi_{5\text{-}1\text{-}2} = -1.6RT_0$. The oxygen transport volumetric coefficient is equal to the calculated value to the Kawase model, based on the surface tension and water column height, along with the molecular oxygen diffusion and viscosity resistance. The maximally increased ratio between oxygen volumetric and drift rate constant, $k_La/k_{dr} = 5.1$ at the $(k_La)_m = (k_La)_K = k_d = k_s$ increases the energy efficiency of oxygen introduction up to $28.4\,gkWh^{-1}$ relative to water column 1 m high, $18.1\,gkWh^{-1}$ where, $k_La/k_{dr} = 3.57$ and $(k_La)_m = (k_La)_K = k_s \leqslant k_d$.

(c) In th regime 5-2-10, oxygen transport volume coefficient is equal to the calculated value to the Calderbank model, $(k_La)_m = (k_La)_C$ based on the viscosity resistance and molecular oxygen diffusion. The decreased over-pressure from 22.3 to 0.061 Pa and electrons density for 30% at anode surface polarization decreased the ratio $k_La/k_{dr} = 2$ and energy efficiency of oxygen introduction two to three times relative to regime 5-2-2.

(d) The twice greater electron densities in the regimes 10-2-*q* relative to 5-2-*q* favour diffusion control of the oxygen introduction, $k_La = k_d$ at 1.4 greater saturation rates constants compared to the diffusion rate constants.

(e) At greater electrons densities and absorption rate constants for one-order of magnitude in the regimes *c*-1-*q*, at twice greater diffusion rates, the saturation rates constants control the oxygen introduction volumetric coefficients, $k_La = k_s$.

References

[1] M. Stanojević, D. Radić, S. Simić, Determining the technical characteristics of the aeration systems for oil refinery's waste water treatment, 16th International Congress of Chemical and Process Engineering, CHISA Praha, Czech Republic, 22 (2004) 3863–3887.

[2] M. Stanojević, S. Simić, D. Radić, A. Jovović, Waste water aeration, ETA, p. 116, ISBN 86-85361-07-09, Belgrade, Serbia (2006).

[3] N.S. Simic, Influence of aeration sistem on the efficiency of the biologycal treatment of the refinery waste water, Ph. D. Thesis, Faculty of Mechanical Engineering, Belgrade, Serbia, 2006.

[4] E. Ashley, K. Hall, D. Mavinic, Factors influencing oxygen transfer in fine pore diffused aeration, University of British Columbia, Water Research, Vancouver (1998) 1479–1486.

[5] K. Fujie, Air diffuser performance in activated sludge aeration tanks, J. Water Pollut. Control Fed., Washington, 1985.

[6] M. Wagner, J. Pöpel, Oxygen transfer and aeration effciency-influence of diffuser submergence, diffuser density and blower type, Water Quality International, IAWQ 19th Biennial International Conference, Vancouver, Canada, 1998.

[7] J. Mc Whirter, J. Hutter, Improved oxygen mass transfer modeling for diffused/subsurface aeration systems, Deparment of Chemical Engineering, The Pennsylvania State University Park, PA 16802, AIChE J, 1989.

[8] J. Dudley, Process testing of aerators in oxidation ditches, Water Res. 29 (9) (1995) 2217–2219.

[9] J. Montgomery, Water Principles and Design, John Wiley & Sons, New York, NY, 1985.

[10] Koichi Fujie, Katsumi Tsuchiya, Liang-Shih Fan, Determination of volumetric oxygen transfer coefficient by of-gas analysis, J Ferment Bioengineer 77 (5) (1994) 522–527.

[11] T.R.E. Treybal, Mass-Transfer Operations, McGraw Hill Book Company, New York, NY, 1981.

[12] H. Hwang, E. Stenstrom, Evaluation of fine bubble alpha factors in near full-scale equipment, J. WPCF 57 (1985) 1142–1151.

[13] G. Degremont, Water Treatment Handbook, fifth ed., Halsted Press/John Wiley's Sons, New York, NY, 1979.

[14] H.J. Rehm, G.W. Schonborn, Biotehnology volume 8, Microbial Degradation, VCH Verlagsgesellschaft mbH, Weinheim, 1986.

[15] OXYFLEX, Membrane diffusers, Kataloge of Bluftungsteehnik, Germany, 1998.

[16] G.M. Masters, Engineering and Science, Introduction to Environmental Engineering and Science, CRC Press/Prentice Hall, Englewood Cliffs, NJ, 1995.

[17] M.M. Ševaljevic, Development of the Galvanostatic Method for Gaseous Arsenic Hydride Generation and Successive Lead and Cadmium Pre-Concentration for Increasing AAS Determination Sensitivity, Ph.D. Thesis, Faculty of Technology, Novi Sad., 2000.

[18] Jelena M. Jakšić, Nedeljko Krstajić, Bane N. Grgur, Milan M. Jakšič, Hydridic and electrocatalytic properties of hypo-hyper –d-electronic combinations of transitions metal intermetallic phases, Int. J. Hydrogen Energy. 23 (1998) 667–681.

[19] M.M. Ševaljević, M. Stanojević, S.N. Simić, M. Pavlović, Thermodynamic study of aeration kinetic in treatment of refinery wastewater in bio-aeration tanks, Desalination 248 (2009) 941–960.
[20] M.M. Ševaljević, S.N. Simić, P.V. Ševaljević, Thermodynamic diagnostic of electron densities in gas bubbles in aerated saturated refinery waste water, Desal. Wat. Treat. 42 (2012) 144–154.
[21] Milutin Obradović, Miladin Krsmanović, Spasoje Đorđrvić, et al, The Chemical and Technological Hand-book, Number 1, Chemical and Physical Data, ed, "Work", Belgrade, 1987, pp. 801–803.
[22] Edwin S. Gould, Inorganic reactions and structure, Standfords Research Institute in Bruklin, Holt, Rinhart and Winston, New York, NY, 1964.